Eur. Phys. J. E (2012) **35**: 17
DOI 10.1140/epje/i2012-12017-x

THE EUROPEAN PHYSICAL JOURNAL E

Regular Article

The transition strength from solid to liquid colloidal dipolar clusters in precessing magnetic fields*

A. Ray and Th.M. Fischer[a]

Institut für Experimentalphysik, Universität Bayreuth, 95440 Bayreuth, Germany

Received 6 October 2011 and Received in final form 31 January 2012
Published online: 9 March 2012

Abstract. We report on the rotation of colloidal clusters of diamagnetic beads and of mixtures of paramagnetic and diamagnetic beads in a ferrofluid in a precessing external magnetic field. The precession angle of the external field is a control parameter determining the stability of the cluster. Clusters become locally unstable when the local precession angle reaches the magic angle. Cluster shape dependent depolarization fields lead to a deviation of the local from the external precession angle such that close to the external magic angle different cluster shapes might coexist. For this reason cluster transitions are weakly or strongly first-order transitions. If the transition is weakly first order a critical speeding up of the cluster rotation is observed. No speeding up occurs for strongly first-order cluster transitions with hysteresis. The strength of the first-order transition is controlled by the size of the core of the cluster.

1 Introduction

The formation of a solid from an assembly of particles is a result of the strength, range and form of attractive particle interactions. In this respect colloidal particles have evolved into a rich model system. The interactions between two pairs of colloids are often known quantitatively and the resulting structure [1,2] can be viewed with microscopic techniques. Amongst the variety of different colloids paramagnetic colloids are one special class of colloids that interact via long-range dipole interactions. The orientation-dependent tensor form of the dipole interactions results in complex static [3] and dynamic [4] structures that can be formed from paramagnetic colloids. Dipole interactions switch from attractive to repulsive depending on whether the magnetic dipole moments are oriented longitudinal or transversal with respect to the particle separation. This orientation dependence of the dipolar interactions can be further exploited by using time-dependent magnetic fields with large Mason number [5] that vary on a time scale too fast for the colloids to relax to their instantaneous equilibrium position [3,6,7]. The colloids therefore experience the time-averaged dipolar interactions. These are attractive in those directions where the frequency of longitudinal orientations of the induced magnetic moment is larger than half the frequency of the two transversal orientations. For an isotropic fluctuation with equal probabilities of longitudinal and the two transversal orientations the average dipole interaction vanishes. One of the simplest time-dependent magnetic fields is a precession of the magnetic field around an axis with precession angle ϑ. For such precession, the frequencies of longitudinal and transversal orientations become similar at the magic angle [8] $\vartheta_{\mathrm{magic}} = 54.7°$ and dipole interactions switch sign. For precession angles below the magic angle the dipole interactions are attractive along the precession axis [9] and repulsive in the plane perpendicular to it. For larger angles we have the opposite behaviour. Dipole interactions are similar for the interaction of diamagnetic particles the magnetic moment of which point in the opposite direction than for paramagnets. Dipole interactions, however, switch sign when one looks at the interaction of paramagnetic and diamagnetic particles. A paramagnet in a precessing field will attract other paramagnets along the precession axis and diamagnets in the plane perpendicular to the precession axis if the precession angle is below magic.

* Supplementary material in the form of an avi file available from the Journal web page at
http://dx.doi.org/10.1140/epje/i2012-12017-x
Supplementary.avi is a movie showing the rotation of the colloidal flowers and diamagnets of figure 1 at precession angles close and far from the magic angle. Top two rows of movies are colloidal flowers. The first row is close to the magic angle. The second row of movies shows the same flowers at a lower angle. Bottom two rows of movies are colloidal diamagnetic clusters. The third row shows the colloidal clusters close to the magic angle, the forth row shows the same colloidal clusters at a higher precession angle. The core size ratio increases for both the colloidal flowers and for the colloidal clusters from the left toward the right. The ratio of the rotation speed of similar flowers and clusters decreases at the same time.

[a] e-mail: thomas.fischer@uni-bayreuth.de

One can prepare effective diamagnetic colloids by immersing non-magnetic colloids, so-called magnetic holes, into a ferrofluid. The interaction of effective diamagnets with paramagnets leads to the formation of flower shaped clusters [10] with a paramagnetic core surrounded by diamagnetic petals. In our present experiments magnetic colloidal holes and paramagnetic colloids are placed in a thin film of ferrofluid between to glass plates. The magnetic ferrofluid glass boundaries give rise to virtual image dipoles suppressing any further attraction of beads of any kind along the film normal and assembly mainly happens in the plane. We assembled different planar clusters of effective diamagnets and of a mixture of effective diamagnets and paramagnetic beads in a ferrofluid film subject to a precessing field. Amongst the clusters formed here we focus on clusters that are isotropic in the film plane. Isotropic clusters of diamagnetic beads form above the magic angle while colloidal flowers with a paramagnetic core surrounded by diamagnets form below the magic angle. Both clusters fall apart when approaching the magic angle from different sides (from above and below, respectively), and the precession angle serves as a control parameter for the stability of the clusters. If the orientation of the magnetic dipoles of each particle were oriented along the direction of the external magnetic field then dipolar interactions would be proportional to the second Legendre polynomial of the precession angle of the external field and therefore continuously decrease to zero when approaching the magic angle. From such a picture one would assume the transition from a cluster toward a colloidal liquid to be of second order. However, the local field at the position of one colloidal particle is a superposition of the external field with the depolarization field resulting from the magnetic moments of the other particles and therefore the local field is generically oriented into a direction different from the external field. An individual particle will hence precess with an angle, different then the precession angle of the external field. The deviation of the local from the external precession angle can self-consistently stabilize or destabilize a certain cluster shape. It is for this reason possible that different structures can be locally stable at the same time. One then observes a coexistence of clusters with a liquid. Depolarization from third particles will therefore in general render the cluster stability/instability transition into a first order transition. The current work focuses on the question of the strength of order of the cluster stability transition. We will show that for clusters consisting of one central core particle and a one-particle thick ring of particles surrounding the core particle, the ratio of the core particle radius to the ring particle radius determines how strongly or weakly the transition is of first order.

A second order transition is a transition where the order parameter changes continuously at the transition. A first order transition exhibits a discontinuous change of the order parameter. The change of one phase to the other occurs via a coexistence of the two phases. The area of the hysteresis measures the dissipated energy when traversing the coexistence region back an forth. Second order transitions are associated with a critical behaviour of response functions as a function of the control parameter, while first order transitions exhibit no critical behaviour.

Here we measure the angular velocity of isotropic colloidal clusters in a ferrofluid that occurs as a response to an external precessing field. As a function of the external precession angle this angular velocity shows a critical speeding up for clusters undergoing a weakly first-order transition to a colloidal liquid with a small hysteresis, while clusters undergoing a strong first-order transition with a large hysteresis show no critical speeding up.

The anisotopic part of the susceptibility tensor of isotropic cluster vanishes such that there is no magnetic torque on the cluster arising due to a preferential orientation of the cluster. The only magnetic torque acting on isotropic clusters is exerted via a memory effect in the contrast of the cluster to surrounding susceptibility. The magnetization in the sample lags behind the magnetic field in both the ferrofluid and in the cluster such that the non-vanishing angle between magnetization and magnetic field results in a magnetic torque in both the ferrofluid and in the cluster. The background torque in the ferrofluid is balanced by the sample wall and the positive or negative excess torque on the cluster results in a steady asynchronous co- or counter rotation of the cluster. The cluster susceptibility of isotropic clusters is a shape-independent isotropic tensor that reflects the interactions that keep the cluster intact. The angular frequency of rotation of the clusters is therefore an ideal measure for the self-consistent interactions that keep the integrity of the cluster.

2 Experimental

For the study of the dynamical behavior of the colloidal flowers and colloidal clusters we used superparamagnetic Dynabeads M-270 functionalized with carboxylic acid (Invitrogen Dynal Oslo, Norway) of diamater $a = 2.8\,\mu$m and effective susceptibility $\chi = 0.8$, non-magnetic carboxylate-coated yellow-green fluorescence polystyrene particles of diameter $2.0\,\mu$m from FluroMax, red fluorescent polystyrene microspheres of diameter $2a = 1.0\,\mu$m from Duke Scientific (Palo Alto, CA) and green fluorescence polystyrene particles with diameters $2a = 3.1\,\mu$m and $2a = 9.9\,\mu$m were obtained from ThermoScientific.

For colloidal flowers the paramagnetic and non-magnetic particles were immersed in diluted ferrofluid EMG 707 FerroTec Ferrosound (FerroTec GmbH, Germany) with controlled proportions (EMG $707 : H_2O = 20 : 80$) depending on the experiment and sandwiched between two cover slips of a separation of roughly $100\,\mu$m. The susceptibility of EMG 707 is $\chi_F = \phi_F \phi_P \chi_{\text{magnetite}}$, with $\chi_{\text{magnetite}} = 21$ the susceptibility of bulk magnetite, $\phi_P = 2\%$ the volume fraction of magnetite nanoparticles in the undiluted ferrofluid and $\phi_F = 1$ ($\phi_F = 0.2$) the volume fraction of ferrofluid in the ferrofluid water mixture. The cover slip was then subjected to static magnetic field, produced by a coil mounted under the sample. Colloidal flowers are formed and these flowers are then placed in a rotating field produced by pairs of Helmholtz coils and was observed with

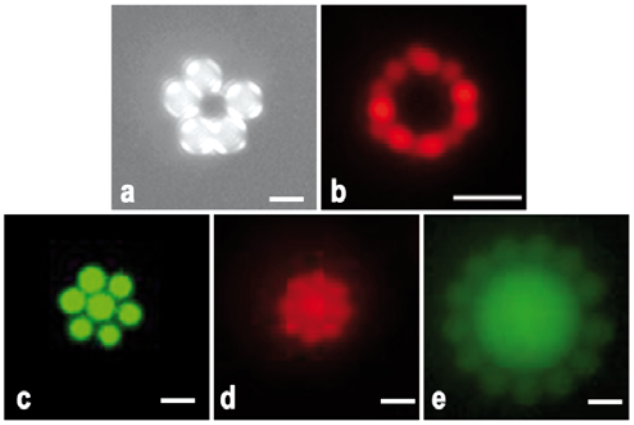

Fig. 1. a)-b) Reflection polarization —respectively, fluorescence— microscope image of a colloidal flower consisting of a paramagnetic (non-fluorescent) core of diameter $2a_1 = 2.8\,\mu$m in an aqueous diluted ferrofluid (EMG707 : $H_2O = 20 : 80$) surrounded by an isotropic ring of diamagnets of diameter a) $2a_2 = 3.1\,\mu$m and b) $2a_2 = 1.0\,\mu$m. The images were obtained in a normal field of $\hat{H}_\perp = 7\,$mT. c)-e) Fluorescence microscope images of isotropic clusters of diamagnets of diameter c) $2a_1 = 3.1\,\mu$m and $2a_2 = 3.1\,\mu$m, d) $2a_1 = 3.1\,\mu$m and $2a_2 = 2.0\,\mu$m and e) $2a_1 = 9.9\,\mu$m and $2a_2 = 3.1\,\mu$m, immersed into an undiluted ferrofluid (EMG 707). The clusters were assembled in an in-plane rotating field of $\hat{H}_\parallel = 1.62\,$mT at a precession angular frequency of $\Omega = 188\,\mathrm{s}^{-1}$. The scale bar in all images corresponds to $3\,\mu$m. The movie in the supporting information shows the rotating clusters under the in-plane field of $\hat{H}_\parallel = 1.62\,$mT and two different normal fields with a precession angle close and far from the magic angle.

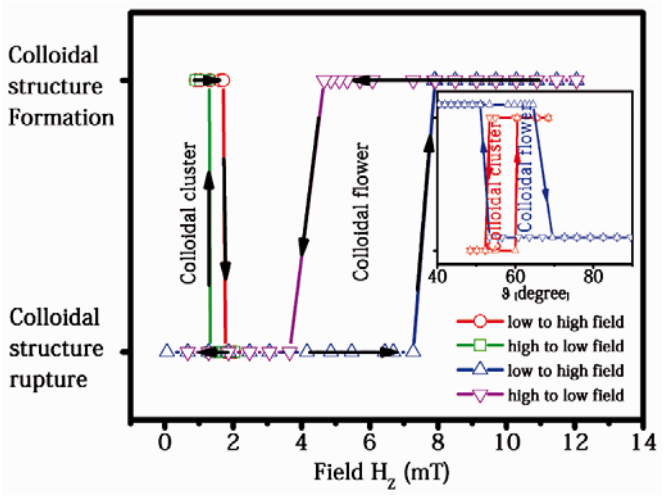

Fig. 2. (Colour on-line) Hysteresis loops of the formation and rupture of colloidal flowers and of diamagnetic clusters as a function of the static normal field $\hat{H}_\perp$. The colloidal flowers consisted of a paramagnetic (non-fluorescent) core of diameter $2a_1 = 2.8\,\mu$m in an aqueous diluted ferrofluid (EMG 707 : $H_2O = 20 : 80$) surrounded by an isotropic ring of diamagnets of diameter $2a_2 = 1\,\mu$m in a rotating field of $\hat{H}_\parallel = 1.62\,$mT at a precession angular frequency of $\Omega = 188\,\mathrm{s}^{-1}$. Blue upward triangles correspond to increasing the normal field and pink downward triangles to decreasing normal field. The diamagnetic clusters consisted of core particles of diameter $2a_1 = 3.1\,\mu$m and petals of diameter $2a_2 = 3.1\,\mu$m immersed in an aqueous undiluted ferrofluid (EMG 707). The rotating in-plane field strength and frequency were the same as for the colloidal flowers. Red circles are measured upon increasing and the green squares upon decreasing the normal field. The inset shows the same hysteresis loops in terms of the precession angle.

fluorescence or reflection microscopy, LEICA DM5000 (Leica Microsystems Wetzlar GmbH, Germany).

For colloidal clusters non-magnetic particles with different size diameters were immersed in undiluted ferrofluid EMG 707 sandwiched between two cover slips. The cover was then subjected to a rotating magnetic field where isotropic colloidal clusters are formed. Then a static magnetic field normal to the film was superposed to the rotating in-plane field and the dynamics of the clusters were observed under the fluorescence microscope.

The field direction of the magnetic field changes from the air into the ferrofluid film according to $\hat{H}_\perp^{\mathrm{ferrofluid}} = \hat{H}_\perp^{\mathrm{air}}/(1+\chi_F)$ and $\hat{H}_\parallel^{\mathrm{ferrofluid}} = \hat{H}_{\parallel\perp}^{\mathrm{air}}$, and the precession angle in the ferrofluid and in the air are related via $\tan\vartheta^{\mathrm{ferrofluid}} = (1+\chi_F)\tan\vartheta^{\mathrm{air}}$. χ_F denotes the magnetic susceptibility of the ferrofluid. All external fields and external precession angles are given in terms of their values inside the ferrofluid.

3 Results

Isotropic colloidal flowers were assembled in a static magnetic field normal to the sample consisting of a mixture of paramagnetic and non-magnetic particles dispersed in a diluted ferrofluid. It has been shown [11,12] that with the proper dilution the magnetic susceptibility can be tuned to prefer a number of diamagnetic petals absorbing at the magnetic core corresponding to a full monolayer of petals around the core. Such kinds of isotropic colloidal flowers are displayed in fig. 1a)-b). Clusters of a bidisperse (radii a_1 and a_2) mixture of effective diamagnets in a ferrofluid were formed in an in-plane rotating magnetic field. The diamagnetic clusters formed are planar clusters lying in the mid plane of the ferrofluid sample having a rich variety of conformations with different numbers of diamagnets forming one clusters. Amongst this variety we picked out clusters having a core formed by a bead of radius a_1 surrounded by a complete monolayer of beads with radius a_2. Examples of such isotropic diamagnetic clusters are shown in fig. 1c)-e).

Both types of clusters were exposed to a precessing magnetic field being a superposition of a rotating magnetic field $\mathbf{H}_\parallel(t) = \hat{H}_\parallel[\mathbf{e}_x\cos\Omega t + \mathbf{e}_y\sin\Omega t]$ in the plane of the ferrofluid film and a static field $\mathbf{H}_\perp(t) = \hat{H}_\perp\mathbf{e}_z$. The precession angle is defined by the ratio of this two components of the field via $\tan\vartheta = \hat{H}_\perp/\hat{H}_\parallel$. The external fields reported are those in the ferrofluid film far away from the clusters. In fig. 2 we show the stability of such

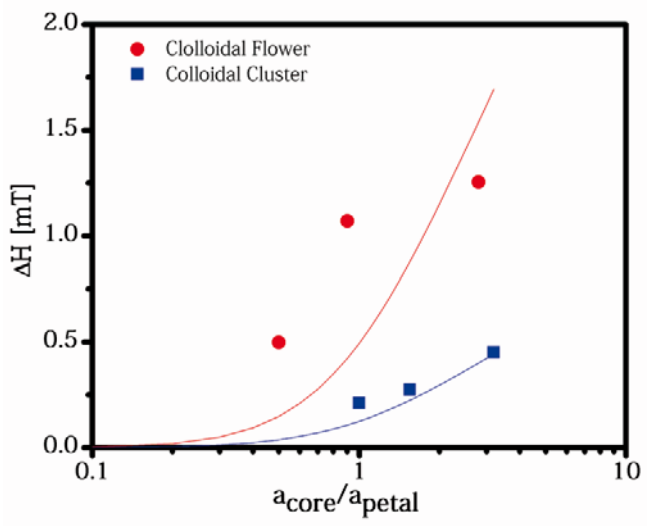

Fig. 3. (Colour on-line) Dependence of the width of the hysteresis loop of the formation and rupture of colloidal flowers (red) and diamagnetic clusters (blue) on the ratio of the core radius and the petal radius. The red and blue lines are fits according to eq. (8).

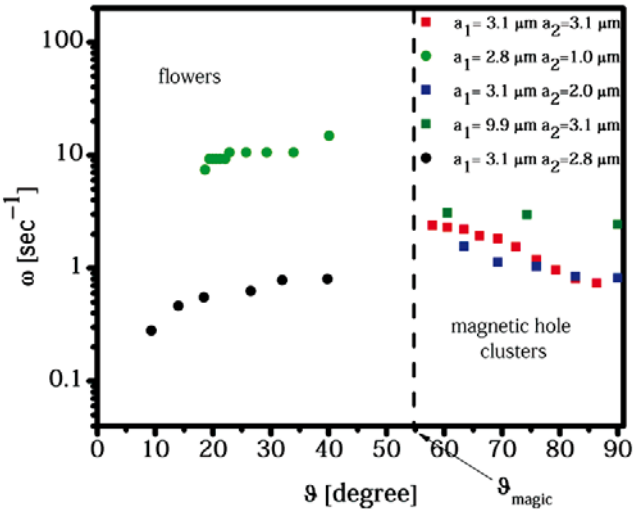

Fig. 4. The angular velocity of different colloidal flowers and diamagnetic clusters as a function of the precession angle recorded at a constant in-plane rotating field of $\hat{H}_{\parallel} = 1.62\,\mathrm{mT}$ at a constant precession angular frequency of $\Omega = 188\,\mathrm{s}^{-1}$.

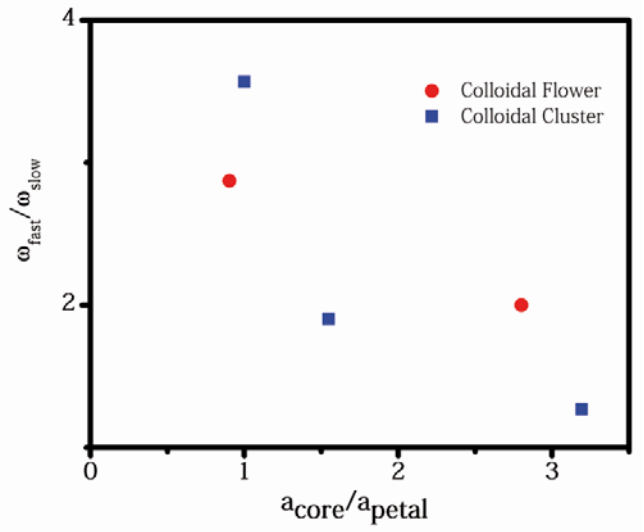

Fig. 5. The angular velocity ratio of different colloidal flowers and diamagnetic clusters near and far from the magic angle as a function of the ratio of the core to the petal radii.

clusters as we sweep the normal component $\hat{H}_\perp$ of the precessing field. Colloidal flowers are stable for low precession angles (large normal field $\hat{H}_\perp$) while clusters of holes are stable at large precession angles (small normal field $\hat{H}_\perp$). Decreasing the normal component of the field destabilizes the colloidal flowers and they fall apart at a critical field $\hat{H}_{\perp c1}$. If we start the experiment at $\hat{H}_\perp = 0$ one observes a mixture of magnetic hole clusters and paramagnetic beads. Colloidal flowers form from this mixture upon surmounting a second threshold $\hat{H}_{\perp c2} > \hat{H}_{\perp c1}$. We characterize the width of this hystersis by the difference of the two critical fields $\Delta\hat{H}_\perp = \hat{H}_{\perp c2} - \hat{H}_{\perp c1}$. The width of the hystersis $\Delta\hat{H}_\perp$ is a measure of how strongly the transition is of first order.

A similar hysteresis is measured when diassembling diamagnetic clusters by increasing the normal component $\hat{H}_\perp$ of the precessing field and reassembling a cluster of a generically different shape and size when decreasing the field. The strength of the transition both for the colloidal flowers as well as for the magnetic hole clusters depends on the size ratio a_1/a_2 of the colloids of the core and of the petals. In fig. 3 we plot the width of the hystersis $\Delta\hat{H}_\perp$ *versus* the size ratio a_1/a_2. The width of the hystersis increases with the size ratio.

The rotating parallel component and the contrast of the imaginary part of the magnetic susceptibility $\Delta\chi''$ of the cluster to the surrounding ferrofluid result in a torque

$$\tau = 4\pi\mu_0\Delta\chi'' V\hat{H}^2\sin^2\vartheta.$$

Here μ_0 is the vacuum permeability, V denotes the volume of the cluster, and $\hat{H}$is the absolute value of the magnetic field. This torque causes the clusters to rotate around their core with an angular frequency $\omega < \Omega$. The ratio $\omega/\hat{H}^2\sin^2\vartheta$ measures how efficient the magnetic field rotation is converted into a rotation of the cluster. In fig. 4 we plot the angular frequency ω at fixed in-plane field strength and frequency as a function of the precession angle ϑ for different clusters. Some of the clusters show a speeding up when one approaches the magic angle [13], where the clusters fall apart. Other clusters do not change their angular frequency when changing the normal component of the field. We characterize the cluster speed up by the ratio $\omega_{\mathrm{fast}}/\omega_{\mathrm{slow}}$, where ω_{fast} denotes the angular frequency just before rupture and ω_{slow} is the angular frequency at low (high) precession angle where the colloidal flower (magnetic hole cluster) is stable.

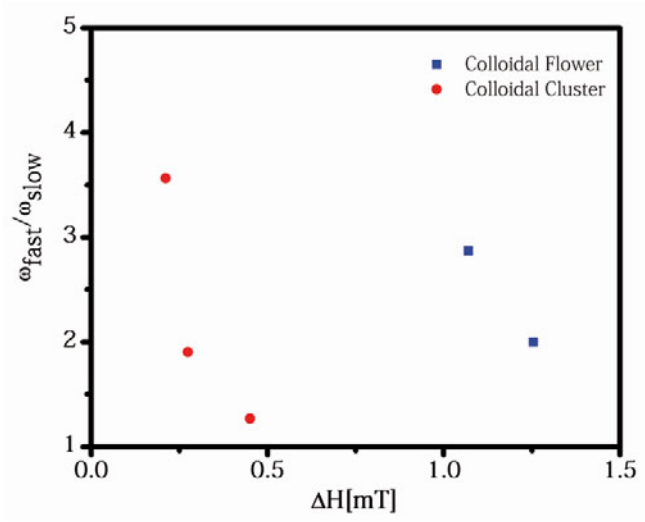

Fig. 6. The angular velocity ratio of different colloidal flowers and diamagnetic clusters near and far from the magic angle as a function of width of the hysteresis.

In fig. 5 we plot the cluster speed up *versus* the size ratio a_1/a_2 of the colloids of the core and of the petals. The speed up decreases with the size ratio for both the colloidal flowers and for the magnetic hole clusters.

Figures 3 and 5 show that both the width of the hystereses and the speed up of the rotation correlate with the ratio of the core-to-the-petal radius $a_{\rm core}/a_{\rm petal}$. We may combine figs. 3 and 5 to measure the speed up as a function of the strength of the first order transition. Hence, in fig. 6 we plot the cluster speed up *versus* the width of the hysteresis. A large speed up is observed for small hysteresis while no speed up occurs at large hysteresis.

4 Discussion

If we consider the core particle to be larger than the particles in the ring it is a good approximation to describe the local magnetic field as that in the absence of the petal particles. Toussaint *et al.* [14] have shown that image dipoles due to the presence of the ferrofluid glass walls can cause a first-order transition with two stable distances between the diamagnets. Here those effects are neglected since the sample thickness is much larger than the separation of the petals from the core. Neglecting the image dipoles, the field from the core is described by

$$\mathbf{H} = \begin{cases} \left[\mathbf{I} + \frac{a_1^3(\chi_c-\chi_F)}{1+\chi_c+2(1+\chi_F)}\frac{3\mathbf{rr}-r^2\mathbf{I}}{r^5}\right]\cdot\mathbf{H}_{\rm ext}, & \text{for } r > a_1, \\ \frac{3(1+\chi_F)}{1+\chi_c+2(1+\chi_F)}\mathbf{H}_{\rm ext}, & \text{for } r < a_1, \end{cases} \tag{1}$$

where $\mathbf{I}$ denotes the unit tensor, and χ_c denotes the susceptibility of the core particle of radius a_1. The effective magnetic moment of the core and petal particles $\mathbf{m}_c = V_c(\chi_c-\chi_F)\mathbf{H}(r=0)$ and $\mathbf{m}_P = V_P(\chi_P-\chi_F)\mathbf{H}(r = a_1+r_2)$ are thus determined by the local field at the particle positions $r = 0$ and $r = a_1 + r_2$, the volumes V_c and V_P of the particles and the susceptibility contrasts to the ferrofluid. The dipolar interaction hence reads

$$W = -\frac{\mu_0}{4\pi}\mathbf{m}_c\cdot\left[\frac{3\mathbf{rr}-r^2\mathbf{I}}{r^5}\right]\cdot\mathbf{m}_P \tag{2}$$

$$= -\gamma\mathbf{H}_{\rm ext}\cdot\left[\frac{3\mathbf{rr}-r^2\mathbf{I}}{r^5} + \frac{a_1^3(\chi_c-\chi_F)}{1+\chi_c+2(1+\chi_F)} \times \left(\frac{3\mathbf{rr}-r^2\mathbf{I}}{r^5}\right)^2\right]\cdot\mathbf{H}_{\rm ext}, \tag{3}$$

where

$$\gamma = \frac{\mu_0}{4\pi}V_PV_c\frac{3(1+\chi_F)}{1+\chi_c+2(1+\chi_F)}(\chi_c-\chi_F)(\chi_P-\chi_F) \tag{4}$$

and $\mathbf{r}$ is the separation vector between the core and petal particle. The first term in (3) corresponds to the interaction of the petal particle in the unperturbed external field and the second term is the perturbation of the magnetic moment of the petal particle due to the presence of the core particle. For an external field $\mathbf{H}_{\rm ext} = H_{\rm ext}(\sin\vartheta_{\rm ext}[\mathbf{e}_x\cos\Omega t+\mathbf{e}_y\sin\Omega t]+\cos\vartheta_{\rm ext}\mathbf{e}_z)$ and a petal particle sitting in the equatorial plane at a distance $r = a_1 + r_2$ the time-averaged dipole interaction energy reads

$$\overline{W} = \frac{1}{2}\frac{\gamma H_{\rm ext}^2}{(a_1+r_2)^3}\left(1+\frac{\beta}{(1+r_2/a_1)^3}\right) \times\left[P_2(\cos\vartheta_{\rm ext}) - \frac{4\beta}{\beta+(1+r_2/a_1)^3}\right], \tag{5}$$

where

$$\beta = \frac{(\chi_c-\chi_F)}{1+\chi_c+2(1+\chi_F)}. \tag{6}$$

The first term in (5) corresponds to a renormalized long-range dipole interaction that scales with second Legendre polynomial $P_2(\cos\vartheta_{\rm ext})$ of the precession angle $\vartheta_{\rm ext}$ and switches sign when passing the magic angle. This part of the interaction is attractive if $(\chi_c-\chi_F)(\chi_P-\chi_F)P_2(\cos\vartheta_{\rm ext}) < 0$ and explains the stability of the colloidal flowers ($\chi_c-\chi_F > 0, \chi_P-\chi_F < 0, P_2(\cos\vartheta_{\rm ext}) > 0$) for small precession angles $\vartheta_{\rm ext} < \vartheta_{\rm magic}$ and the stability of the diamagnetic clusters ($\chi_c-\chi_F < 0, \chi_P-\chi_F < 0, P_2(\cos\vartheta_{\rm ext}) < 0$) for large precession angles $\vartheta_{\rm ext} > \vartheta_{\rm magic}$. The second term is independent of the precession angle. Its sign does not depend on the sign of the susceptibility contrast $\mathrm{sign}(\chi_c-\chi_F)$ of the core particle to the ferrofluid. The second term is repulsive for petal particles that are magnetic holes ($\chi_P-\chi_F < 0$), while for paramagnetic particles it is attractive. The destabilizing correction term is short range. This results in an equilibrium distance of the petal from the core given by

$$r_{2,\rm min} = a_1\left[\sqrt[3]{\frac{4\beta}{P_2(\cos\vartheta_{\rm ext})}-\beta}-1\right], \tag{7}$$

that moves from infinity at the magic angle $\vartheta_{\rm ext} = \vartheta_{\rm magic}$ toward the hard-core distance a_2 as one moves away from

the magic angle. The picture changes when the dipole interactions between the petals are taken into account as well. Here the different range of both interactions becomes important when summing up the interaction of all petal particles. We expect that in a cluster of N particles that the dipole interaction increases with the number of pairs of particles that scales as N^2, while the short-range correction increases with the number of nearest neighbor particles that scales like N. This explains the hystereses since once a cluster is formed it can be stabilized by the long-range dipole interactions even when a single pair of particles is not yet stable. The minimum radius of N petals will hence be different from that of one petal described by eq. (7). We expect the hystereses to roughly scale with the ratio of the long-range to short-range interactions such that

$$\Delta H \propto 1/(\beta + (1 + a_2/a_1)^3). \quad (8)$$

In fig. 3 we have incorporated curves according to eq. (8) with the prefactor of eq. (8) fitted to the data. The fit agrees well for the colloidal cluster but is less accurate for the colloidal flowers. This is not too suprising since the different susceptibility of the core of the flower adds to the complexity of the phenomenon. The width of the hystereses is a measure for the strength of the first-order transitions. If the transition is weakly first order, some of the second-order critical phenomena are likely to persist. This is what we observe in the critical speeding up. For a second-order transition we would expect the rotation speed of the cluster to diverge. For a weakly first-order transition there is significant increase when approaching the transition, while no significant increase is observed when the transition is strongly first order. The interaction between particles at the magic angle in an isotropic environment vanishes. Some interaction will persist if the larger size of the core renders the environment anisotropic. The self-consistent deviation of the system from isotropic is what stabilizes or destabilizes the particular conformation and renders the transition from second to first order. It is therefore conceivable that the presence of a large core particle is responsible for the strong first-order type of transitions in the clusters with a large core. The corresponding second-order speeding up of the rotation of the cluster is destroyed by the large core and partially persists for smaller core sizes.

5 Conclusions

The rotation of colloidal clusters of non-magnetic holes and of mixtures of paramagnetic beads with non-magnetic holes in a ferrofluid in a precessing external magnetic field depends on the precession angle of the external field that serves as a control parameter for the stability of the clusters. Near the magic angle cluster-shape–dependent depolarization fields cause an orientation of the local field deviating from the external field and render cluster transitions weakly or strongly first order. If the transition is weakly first order a critical speeding up of the cluster rotation is observed. No speeding up occurs for strongly first-order cluster transitions with hysteresis. The strength of the first-order transition is larger the larger the size of the core as compared to the petal particles of the cluster.

This work is supported by the German Science Foundation within the cluster of excellence SFB840.

References

1. P. Pieranski, Contemp. Phys. **24**, 25 (1983).
2. A. vanBlaaderen, R. Ruel, P. Wiltzius, Nature **385**, 321 (1997).
3. James E. Martin, Eugene Venturini, Gerald L. Gulley, Jonathan Williamson, Phys. Rev. E **69**, 021508 (2004).
4. N. Casic, S. Schreiber, P. Tierno, W. Zimmermann, Th.M. Fischer, EPL **90**, 58001 (2010).
5. A.P. Gast, C.F. Zukoski, Adv. Colloid Interface Sci. **30**, 153 (1989).
6. N. Osterman, I. Poberaj, J. Dobnikar, D. Frenkel, P. Ziherl, D. Babic, Phys. Rev. Lett. **103**, 228301 (2009).
7. G. Helgesen, P.O. Pieranski, A.T. Skjeltorp, Phys. Rev. A **42**, 7271 (1990).
8. E.R. Andrew, A. Bradbury, R.G. Eades, Nature **182**, 1659 (1958).
9. J. Cernak, G. Helgesen, A.T. Skjeltorp, Phys. Rev. E **70**, 031504 (2004).
10. R.M. Erb, H.S. Son, B. Samanta, V.M. Rotello, B.B. Yellen, Nature **457**, 999 (2009).
11. K.H. Li, B.B. Yellen, Appl. Phys. Lett. **97**, 083105 (2010).
12. A. Ray, S. Aliaskarisohi, Th.M. Fischer, Phys. Rev. E **82**, 031406 (2010).
13. P. Tierno, R.M. Muruganathan, Th.M. Fischer, Phys. Rev. Lett. **98**, 028301 (2007).
14. R. Toussaint, J. Akselvoll, G. Helgesen, A.T. Skjeltorp, Phys. Rev. E **69**, 011407 (2004).